

# BRAZIER EFFECT IN SPINNING HOLLOW COMPOSITE DRIVE SHAFT USING MIXED FINITE ELEMENT METHOD

Pramod Kumar<sup>†</sup> and Dineshkumar Harursampath<sup>‡</sup>  
 Department of Aerospace Engineering, Indian Institute of Science  
 Bangalore-560012, INDIA

## Abstract

The objective of the present work is to present a unified analysis which will take into consideration the effect of non linearity between the bending moment and curvature in long composite drive shaft which become important at high speeds even while transmitting uniform torque. Weak formulation used here is the well-established version of the nonlinear dynamics of moving beams developed by Hodges. The shaft is modeled as a spinning tubular beam using the non-linear cross-sectional stiffness matrix, which captures the brazier effect in an asymptotically correct manner. The critical speed of the thin-walled composite shaft is dependent on the stacking sequence, the length-to-radius ratio (L/R) and the boundary conditions. The present analysis is verified by comparing the numerical results with those in the literature and very good agreement is obtained. Both forward and backward precession mode shapes are also captured for spinning drive shafts.

## Nomenclature

$\mathbf{b}_i$	unit vectors of undeformed beam
$\mathbf{B}_i$	unit vectors of deformed beam
$C$	direction cosine matrix
$F$	column vector containing the axial ( $F_1$ ) and shear forces ( $F_2$ and $F_3$ )
$f, m$	external forces and moments
$H$	cross-sectional angular momentum
$I$	section inertia matrix
$K$	deformed beam curvature
$l$	length of shaft
$M$	column matrix of torsional moment ( $M_1$ ) and bending moments ( $M_2$ and $M_3$ )
$P$	cross-sectional linear momentum
$R$	mean radius of shaft
$S_{33}$	nonlinear bending stiffness
$t$	wall thickness of shaft
$u$	column matrix of displacement measures
$V$	inertial velocity vector
$\gamma$	column vector of beam axial and transverse shear strains
$\kappa$	column vector of beam torsional ( $\kappa_1$ ) and bending ( $\kappa_2$ and $\kappa_3$ ) curvatures
$\rho$	bending curvature (either $\kappa_2$ or $\kappa_3$ )
$\Omega$	inertial angular velocity vector
$\theta$	column matrix of Rodrigues parameters
$\Delta$	Identity matrix

$\mu$	beam mass per unit length
$\delta u, \delta \theta$	virtual quantities
$(\cdot)', (\dot{\cdot})$	spatial and temporal derivatives

## Introduction

Fiber reinforced shafts have been sought as new potential candidates for replacement of the conventional metallic shafts in many applications like commercial drive shafts, for helicopter rotors, aircraft propellers, and inboard motor propellers for luxury yachts and fishing boats. They are gaining lot of popularity because of their many advantages over metallic shafts like significant weight reduction, reduced bearing and journal wear, assured dynamic balance with symmetric layups and increased operating speeds, tailorability of electrical conductivity, corrosion resistance, reduced noise, vibration and harshness (NVH) and long fatigue life. This in short means improved performance of the shaft system resulting from the use of composite materials. In many engineering systems, we have to design rotating members which are capable of smooth operations under various conditions of speed and load. In some systems, specially for machinery with members rotating at high speeds, it is extremely difficult to ensure stable and smooth operation. Although this subject is still in the developing stage, nevertheless, because of its importance, it is necessary for designers to have some understanding of the behavior of rotating members. The motivation for reviewing models for critical speed comes from the Brazier effect (i.e the non-linear behavior of thin tube in bending). Critical speed which is a function of bending stiffness which reduces with increasing bending curvature. This effect becomes very important at high spinning speed in helicopter drive shafts. Earlier researchers studied the dynamics of shafts by considering a linear cross-sectional analysis and a non-linear beam analysis through the longitudinal direction.

Most of the shaft models in the literature are based either on the shell theories, on beam theories combined with strain-displacement relation of shell theories or on thin walled beam theories. One of the main difficulties sprouts from the large variety of structural responses of a general shell, depending on its geometric shape, on the applied loads and the boundary conditions. A reliable shell finite element must capture all possible behavior of the structure. Generally composite shafts are thin tubular shafts, and thus, studying cross-sectional deformation both inplane and out-of-plane is important. Most of the formulations based on beam theories fail to predict shaft cross-section deformation. Though, formulations based on shell elements are most suitable for studying shaft cross-

<sup>†</sup>Research Scholar

<sup>‡</sup>Assistant Professor, Corresponding Author, Tel: 91-80-22933032, Fax: 91-80-23600134, E-mail:dinesh@aero.iisc.ernet.in

sectional deformation, they are computationally costlier compared to beam formulations. Hence, the optimal approach would be to use a thin-walled beam theory based on a rigorous shell theory.

The dynamic analysis of rotor-bearing systems for isotropic shafts has been covered by many researchers 1-6. Literature survey shows that there are few models developed for the anisotropic shafts. In literature, the bulk of the work on cylindrical shell is on non rotating shells. The work of Greenberg and Stavsky 7, for example, presents the vibration analysis of non-rotating laminated composite cylindrical shells. Accompanied by the development of many new advanced composite materials, various mathematical models of spinning composite shafts were developed by researchers. Rand and Stavsky 8 studied the dynamic characteristics of rotating laminated filament-wound cylindrical shells by using a closed-form solution of a general type of field equations and arbitrary boundary conditions. Kim and Bert 9 have presented the most significant work related to the whirling of composite drive shafts including the bending-twisting coupling and transverse deformations. They have shown that in the case of relatively short shafts, transverse shear deformation can be important. Singh and Gupta 10 presented two composite spinning shaft models based on an EMBT (Equivalent Modulus Beam Theory) and a layerwise theory. Chen and Peng 11 studied the stability of rotating composite shafts under axial compressive loads. Most recently Chang *et.al.* 12 developed a simple laminated composite shaft model based on a first order beam theory. They assumed that the composite shaft is supported by bearings, which was modeled as springs and dampers. They derived the governing equations of systems starting from Hamilton's principle.

As a thin walled circular cylindrical shell is subjected to bending deflection, it will tend to ovalize according to Brazier effect 13. In doing so, the diminishing cross-sectional second moment of area of the tube reduces the flexural stiffness of the structure. This effect was captured by Harursamath and Hodges 14 for long anisotropic tubes. The Variational Asymptotic Method (VAM) 15 was used to find the one dimensional strain energy of the beam. This tool (VAM) is a powerful mathematical tool which takes a long 3-D body and represents it as a 1-D body motivated by some small natural parameters arising from the geometry itself. In the case of thin-long tubes, the radius-to-length ( $R/l$ ) and thickness-to-radius ( $t/R$ ) ratios may be considered as small parameters. No adhoc assumption is taken into consideration. However, the strains are assumed to be small though large deformations are allowed. Starting from the Classical Laminated Shell Theory (CLST), VAM was used to obtain a beam theory, for circumferentially uniform stiffness tubes, which captures the Brazier effect analytically.

A non-linear formulation for the dynamics of initially curved and twisted beams in a moving frame 17 is used for this analysis. These equations are written in a compact matrix form without any approximation to the geometry of the deformed beam reference line. Earlier, Danielson and

Hodges 18, have expressed the 3-D strain field in the beam in terms of one dimensional generalized strains. These relations were used to derive the intrinsic equation from Hamilton's principle where one dimensional strain energy per unit length was taken from the expressions derived in 14. These equations are most simple in their intrinsic form and can be conveniently cast in a mixed finite element 19 form.

Analysis is carried out after modeling to determine the dynamics of spinning composite drive shafts taking into consideration the Brazier effect which is then shown to be important for high speed spinning shafts. Clamped-clamped boundary condition is considered for the drive shaft. Modal analysis is done for composite drive shafts both under non-rotating and rotating conditions. Influence of Brazier effect in shaft transmitting uniform torque is taken up for study. Analysis shows that earlier theories fail to capture the Brazier effect which becomes important at high speed spinning conditions.

### Cross-sectional analysis

Calculation of natural frequencies for a composite beam requires two different operations. These two different operations together represent the three dimensional modelling of composite beams by combining efficiency with accuracy. The first one is the determination of non-linear cross-sectional stiffness by solving the two dimensional cross-sectional problem for use in the non-linear one dimensional equation by using variational asymptotic analysis. The second one is the solution of the one dimensional beam equation for the natural frequencies and mode shapes. Here, the objective is to study how the non-linear changes in stiffness affect the dynamics characteristics of the beam. Asymptotically correct beam model derived by Harursamath 14 for a long, thin-walled, circular tube with circumferentially uniform stiffness (CUS) and made of fiber reinforced materials was derived.

The final expression for the beam strain energy density of composite tube as given in 14 is

$$U_{1D} = \frac{1}{2} \begin{Bmatrix} \gamma_{11} \\ \kappa_1 \\ \rho \end{Bmatrix}^T \times \begin{bmatrix} 2\pi R A_{11} & -2\pi R^2 A_{16} & 0 \\ -2\pi R^2 A_{16} & 2\pi R^3 A_{66} & 0 \\ 0 & 0 & S_{33}(\rho) \end{bmatrix} \begin{Bmatrix} \gamma_{11} \\ \kappa_1 \\ \rho \end{Bmatrix} \quad (1)$$

where

$$S_{33}(\rho) = \pi R^3 A_{11} \left[ 1 - \frac{9(R\rho)^2}{144\mu + 10(R\rho)^2} \right] \quad (2)$$

As expected, due to circular symmetry of the tube, there is no bending-torsion or bending-extension coupling. Hence, extension-torsion and bending could be treated as two independent problems for spanwise uniform, CUS tubes made of generally anisotropic material. Fig.(2) shows that even for a small range of  $\rho$  the second term in Eq.(2) for  $S_{33}$  reduces the bending stiffness with increasing bending curvature and is the source of the well-known non-linearity.

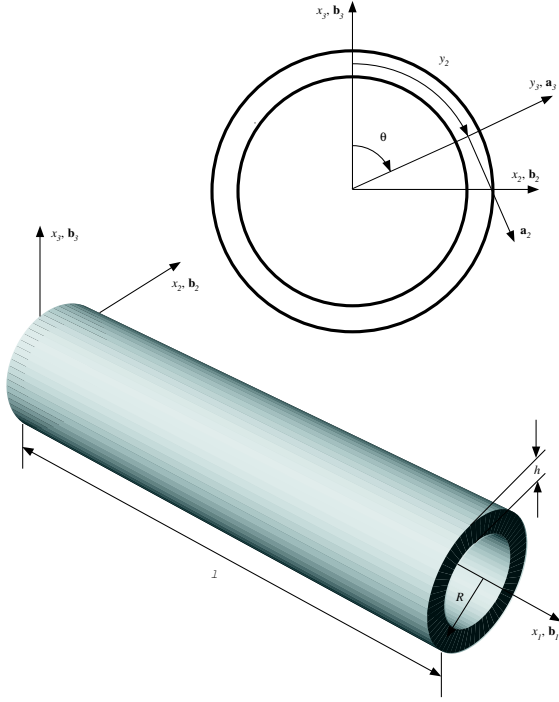


Fig 1. Coordinate systems

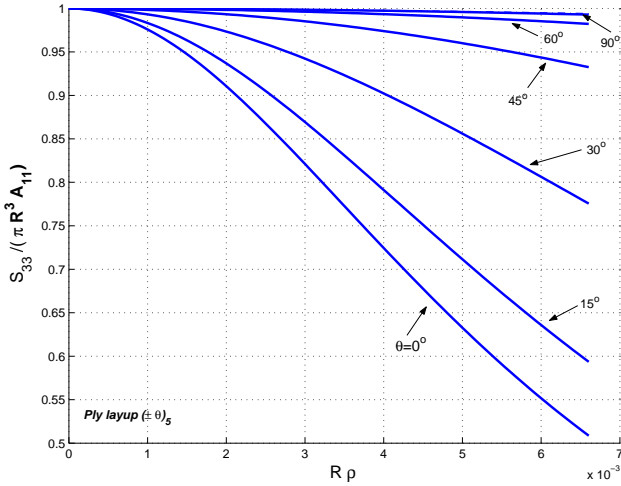


Fig 2.  $S_{33}$  vs curvature of beam

Its reduction is more prominent for the case of the lower value of  $\theta$ , layup considered is  $[\pm\theta_5]$ . As seen in Eq. (2), the only factor influencing this non-linearity is the ratio of the square of the non-dimensional bending curvature,  $R\rho$ , to  $\mu = \frac{D_{22}}{R^2 A_{11}}$ . The definition of  $\mu$  shows that it is a non-dimensional measure of the resistance of the cross section to flatten/deform in its own plane. A small  $\mu$  results in a cross section which is very easily deformed causing highly non-linear behavior. The limiting cases are:  $\mu = 0$  which results in a semi-membranous (infinitesimally thin) tube with 90% reduction from the linear value of  $S_{33}$  independent of the bending curvature; and  $\mu = \infty$  which results in a rigid cross section tube with no non-linearity.

## Weak formulation and mixed finite element method

Beam theory in terms of nonlinear intrinsic strain measures  $\gamma$  and  $\kappa$  were developed by many researchers [16,17,18]. Beam reference line strain and curvatures are denoted by

$$\gamma = \begin{pmatrix} \gamma_{11} \\ 2\gamma_{12} \\ 2\gamma_{13} \end{pmatrix}, \quad \kappa = \begin{pmatrix} \kappa_1 \\ \kappa_2 \\ \kappa_3 \end{pmatrix}, \quad (3)$$

The six generalized strain measures,  $\gamma_{ij}$  and  $\kappa_i$ , functions of the displacement measures,  $u$  of the beam reference line and the relationship between orthogonal base vectors,  $b_i$  and  $B_i$ , of the deformed and undeformed configuration. Then strain measures can be defined 17 as

$$\gamma = C(\mathbf{e}_1 + \mathbf{u}'_b) - \mathbf{e}_1 \quad (4)$$

The components of  $C_{ij}$  are direction cosine and define by

$$C_{ij} = \mathbf{B}_i \mathbf{b}_j \quad (5)$$

$$\kappa = K_B \quad (6)$$

where the elements of the curvature vectors are define by the skew symmetric matrix

$$\tilde{K}_B = -C' C^T. \quad (7)$$

Here  $(\ )'$  denotes the derivative with respect to  $x_1$ ,  $\mathbf{e}_1 = [1 \ 0 \ 0]^T$  and  $\tilde{(\ )}$  denotes a skew symmetric matrix. Angular velocity as defined in Kane and Levinson 16 for the dual basis system is

$$\tilde{\Omega}_B = -\dot{C} C^T \quad (8)$$

Linear velocity in the B basis can be defined as

$$V_B = C \dot{u}_b \quad (9)$$

Detailed derivation of the dynamics of a moving beam can be found in 17. Weak formulation used here is the linearized mixed version of the mixed, weak formulation derived in 19. The equations are written in a compact matrix form without any approximations to the geometry of the deformed beam reference line or to the orientation of the intrinsic cross-section frame. The formulation is in the weakest possible form because all the one dimensional field equations, namely equilibrium equations, constitutive law, strain displacement relationships and boundary conditions are represented in the most basic form without differentiation of any field variable with respect to the axial coordinates. Although this formulation generates a large vector of unknowns the coefficient matrix is very sparse ensuring computational efficiency. For small strain, constitutive equations implied in 17 are written here in the form

$$\begin{Bmatrix} \gamma \\ \kappa \end{Bmatrix} = \begin{bmatrix} R & S \\ S^T & T \end{bmatrix} \begin{Bmatrix} F \\ M \end{Bmatrix} \quad (10)$$

Similarly, the generalized momentum-velocity relations are

$$\begin{Bmatrix} P \\ H \end{Bmatrix} = \begin{bmatrix} \mu \Delta & 0 \\ 0 & I \end{bmatrix} \begin{Bmatrix} V \\ \Omega \end{Bmatrix} \quad (11)$$

Here  $I$  and  $m$  are the section inertia and mass matrices respectively. The governing equation 19 of the dynamics of a moving beam with the reference axis coincides with the axis of mass center is

$$\begin{aligned} & \int_0^l (\delta u'^T C^T F_B + \delta \psi'^T C^T M_B - \delta \bar{\psi}'^T C^T (\tilde{e}_1 + \tilde{\gamma}) F_B \\ & + \delta u^T (C^T P_B) \cdot + \delta u^T \tilde{\omega} C^T P_B + \delta \bar{\psi}^T (C^T H_B) \cdot \\ & + \delta \bar{\psi}^T \tilde{\omega} C^T H_B + \delta \bar{\psi}^T C^T \tilde{V}_B P_B - \delta \bar{F}^T [C^T (e_1 + \gamma) \\ & - e_1] - \delta \bar{F}'^T u - \delta \bar{M}^T (\Delta + \frac{\tilde{\theta}}{2} + \frac{\theta \theta^T}{4}) \kappa - \delta \bar{M}'^T \theta \\ & + \delta \bar{P}^T (C^T V_B - v - \tilde{\omega} u) - \delta \bar{P}^T \dot{u} + \delta \bar{H}^T (\Delta - \frac{\tilde{\theta}}{2} \\ & + \frac{\theta \theta^T}{4}) (C^T \Omega_B - \omega) - \delta \bar{H}^T \dot{\theta} - \delta u^T f - \delta \bar{\psi}^T m) dx_1 \\ & = (\delta u^T \hat{F} + \delta \bar{\psi}^T \hat{M} - \delta \bar{F}^T \hat{u} - \delta \bar{M}^T \hat{\theta}) \end{aligned} \quad (12)$$

In Eq.(12), there are no spatial derivatives of any unknowns and hatted terms indicates the boundary terms. This equation represents the weakest possible form for analyzing the non-linear structural dynamics of a beam as an eigenvalue problem. Eq. (12) is solved by mixed finite element method for natural frequencies and modal solutions.

Since above formulation is already in the weakest form, simple shape functions can be used and the beam discretized into  $N$  elements (see Fig.(3)) with nodes numbered from 1 to  $1 + N$ . We can use the shape functions 19 for defining the virtual displacement, rotation, forces and moments as

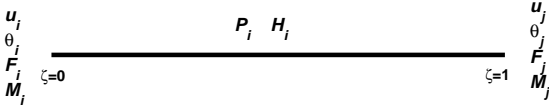


Fig 3. Beam element with unknowns

$$\begin{aligned} \delta u &= \delta u_i(1 - \zeta) + \delta u_j \zeta \\ \delta \theta &= \delta \theta_i(1 - \zeta) + \delta \theta_j \zeta \\ \delta F &= \delta F_i(1 - \zeta) + \delta F_j \zeta \\ \delta M &= \delta M_i(1 - \zeta) + \delta M_j \zeta \end{aligned} \quad (13)$$

where subscripts refer to node number along the beam and  $\zeta$  is a local element axial coordinate so that  $0 \leq \zeta \leq 1$ . The unknowns corresponding to the remaining two virtual quantities ( $P_i$  and  $H_i$ ) are assumed to be piece-wise constant within the element ( $0 < \zeta < 1$ ).

The formulation is termed as mixed, since the unknown include  $u$ ,  $\theta$ ,  $F$ ,  $M$ ,  $P$  and  $H$  (where  $u$ ,  $\theta$ ,  $F$ ,  $M$ ,  $P$  and  $H$  are the displacement, rotation, forces, moments, linear-momentum and angular-momentum, respectively) at each node or for each element. Above discretization seems to be crude but is sufficient for the weakest mixed, intrinsic formulation. In this analysis, we have used equally space elements. Substituting Eq. (13) in the Eq. (12) and recognizing independent of the remaining virtual quantities

results in sets of 30 equations 19. Eq.(12) yields a group of equations which can be written in operator form as

$$Z(X, \dot{X}, \bar{F}) = 0 \quad (14)$$

where  $X$  is the vector of unknowns and  $Z$  is a vector of functions.  $\bar{F}$  is a vector containing the effective nodal loads. Both  $X$  and  $Z$  are of dimensions  $18N + 12$ . In the case of a clamped-clamped boundary condition, the unknown vector will be

$$\begin{aligned} X^T &= [\hat{F}_1^T \hat{M}_1^T u_1^T \theta_1^T F_1^T M_1^T P_1^T H_1^T \dots \\ & u_N^T \theta_N^T F_N^T M_N^T P_N^T H_N^T \hat{F}_{N+1}^T \hat{M}_{N+1}^T] \end{aligned} \quad (15)$$

$Z$  consists of the corresponding terms of Eq(14) and forms the set of nonlinear equations. Set of  $18N + 12$  non-linear equations can be solved by applying the Newton-Raphson method. Using the standard finite element technique, the resulting algebraic equations (Eq.(14)) can be written in matrix form for each element as a first order differential equations in the following form

$$[M] \{ \dot{X} \} + [N] \{ X \} = \{ \hat{F} \} \quad (16)$$

The above equation governs the dynamic response of the system. Here the matrices  $[M]$  and  $[N]$  are defined as

$$[M] = \frac{\partial Z}{\partial \dot{X}}, [N] = \frac{\partial Z}{\partial X} \quad (17)$$

while  $\hat{F}$  contains the dynamic components of external loads. Advantage of the above formulation is that the Jacobian of Eq.(14) can be obtained explicitly and the matrices defined above are tremendously sparse that ensuring the computationally efficiency, without loss of accuracy.

Using the standard finite element technique, resulting algebraic equation can be written in matrix form for each element. These matrices can then be assembled producing one large matrix equation where it can be seen that the final coefficient matrix is simply a reorganization of individual coefficient matrices which is unlike the displacement formulation where the method requires additions during assembly. Separating variables according to whether their time derivative appears or not in Eq.(16), we can rewrite the governing equation as

$$\begin{bmatrix} A & B \\ C & D \end{bmatrix} \begin{Bmatrix} x_d \\ x_s \end{Bmatrix} + \begin{bmatrix} 0 & 0 \\ E & 0 \end{bmatrix} \begin{Bmatrix} \dot{x}_d \\ 0 \end{Bmatrix} = \begin{Bmatrix} 0 \\ 0 \end{Bmatrix} \quad (18)$$

where  $x_d$  is the subset of the field variables which are differentiated with respect to time,  $x_s$  are the rest of the field variables,  $A, B, C$  and  $D$  are coefficient matrices and  $f_d$  and  $f_s$  are the external forces. It must be noted here that this is a very sparse matrix equation. Also the matrix  $D$  always contains nonzero diagonal, no matter how many elements are used. After solving the above two equations for free vibration analysis by eliminating  $x_s$ , the matrix equation can be ultimately reduced to an eigenvalue problem is defined by

$$-BD^{-1}E\dot{x}_d + (A - BD^{-1}C)x_d = 0 \quad (19)$$

Above algebraic eigenvalue problem is of the order of  $12N$  and can be used to calculate the vibration characteristics of the beam. Several methods can be used to determine the critical speed of a rotating drive shaft. They include commonly known Campbell diagram method as well as whirling frame method (suitable for undamped system) and sensitivity method. Eq. (19) is solved for increasing values of spinning speed that result in bifurcation of natural frequencies into two sets of roots. One will increase with increasing spinning velocity (called forward precision) and the other will decrease (called the backward precision). For long shafts, these roots are very close to each other.

### Stability of rotating shafts

Zenberg and Simmonds 20 analyzed a composite shaft both theoretically and experimentally with 10 layers and at different fiber angles. The critical speed was found by using a finite element beam formulation in which beam element was derived based on Donnell's shell theory by Dos Reis et. al 21. These results also take into consideration the bending-stretching coupling effects. In the presents analysis, the results for the shaft were obtained by using the stiffness matrix which is non-linear under bending. A comparison of results is given in Table II. It may be noted that, because of the non-linear behavior of thin tube against curvature, critical speed reduces with increasing bending curvature. This effect is prominent for higher modes. The critical speed predicted by Zinberg and Symmond using EMBT is 5780 rpm and natural frequency of the shaft was experimentally found to be 5500 rpm from the forced response of the non rotating shaft. Using the present analysis the critical speed turns out to be 5195 rpm, close to the theoretical analysis of Zinberg and Symmond. Earlier researchers have not taken into consideration the deformation of the cross section to an oval shape which reduces the flexural stiffness. But it has been found that at first critical speed, cross-sectional deformation is negligible. Therefore, it will not affect the solution significantly.

In the following example, first critical speeds of composite shafts are determined for various layups and compared with those available in the literature to validate the present model. For thin walled shafts with a given orientation  $\pm\theta$ , the second moment of inertia which is used in the expressions for the flexural stiffness is approximately proportional to  $t$ , the thickness of the tube wall. Therefore inplane modulus can be used for calculation of flexural stiffness. During the flexural modes, one half portion of the tube is in compression and other half will be in tension. Thus the direction of stretching force induced in the mid-surface of the tube wall is opposite in the two halves. Similarly, in case of tension in CUS composite shafts, the induced bending moment due to bending-stretching coupling will be symmetric about the cross section and will not cause any flexure in the tube. Therefore, although the bending-stretching coupling can be present in lamination construction, will not not affect the bending behavior of the CUS tube. In conventional beam analysis, it is also assumed that plane section remain plane after bending and the shape of the cross section is

not deformed. However in reality and in the current model, the cross section also deforms during bending, which can affect the bending mode natural frequencies significantly. For numerical simulation, the layup  $[\pm\theta]_5$  with all 10 plies of equal thickness and following properties is considered.

	Boron/ Epoxy	Graphite/ Epoxy
$E_1$ (GPa)	211	139
$E_2$ (GPa)	24.1	11.0
$\nu_{12}$	0.36	0.313
$G_{12} = G_{13}$ (GPa)	6.90	6.05
$G_{23}$ (GPa)	6.90	3.78
$\rho$ (Kg/m <sup>3</sup> )	1967	1578

TABLE I  
PROPERTIES OF COMPOSITE MATERIAL USED.

### Variation of critical speed with ply orientation

The critical speeds calculated using present analysis are plotted w.r.t. ply orientation in Figs. (6) and (7). In Fig.(6), the first critical speeds are plotted w.r.t. to ply angle for  $t/R = 1/50$  ( $t$  is the thickness of the laminate,  $R = 6.605$  cm, the mean radius of the shaft). From Fig.(6), it is noted that the first critical speed for clamped-clamped boundary condition is almost constant in the range  $0^\circ \leq \theta \leq 15^\circ$  and then decreases as we increase the ply orientation. The bending rigidity is large in the range  $\theta = 0^\circ - 15^\circ$  and then reduces with increase in the ply orientation of fibers. This is a combined result of many known phenomenon. The shear modulus is maximum at  $45^\circ$  and minimum at  $0^\circ$  and  $90^\circ$ . Also longitudinal modulus is maximum at  $0^\circ$  and minimum at  $90^\circ$ . Shear deformation in beam reduces the natural frequency and will be prominent for large value of longitudinal modulus and smaller value of shear modulus. As the ply angle changes from  $0^\circ$  and  $90^\circ$ , it thus reduces the critical speed. Also the shear modulus increases from  $0^\circ$  to  $45^\circ$ , leading to reduce the shear deformation effect, which in turn increases the critical speed. The latter effect dominates for smaller value of  $L/R$  ratio. If we compare the two plots, it is found that in Fig.(7), the maximum critical speed is shifted towards the higher angles for lower value of  $L/R$  ratio.

### Variation of the critical speed with $L/R$ and $t/R$

This section illustrates the variation of the critical speed with respect to  $L/R$  and  $t/R$ . As discussed earlier, the shear modulus tends to shift the peak towards the higher ply angle and is shown in Fig.(8) also. Critical speed reduces at a rate faster with increasing  $L/R$  (Fig. 8(a)) as compared to the case of increasing  $t/R$  (Fig. 8(b)). It is found that critical speeds is less sensitive to  $t/R$  ratio because the cross-sectional deformation is negligible for thicker shafts.

### Spinning drive shaft under the action of external forces/disturbances

This section considers the composite drive shaft transmitting uniform torque. Transmitted force at the shaft periphery is resolved into a transverse force and a torque acting through the centroidal axis. In the following example, we consider the composite drive shaft under the action of external force/disturbance both with and without Brazier effect. Graphite/ Epoxy shaft with of  $R=0.0605$  m;  $R/t=50$  and  $L/R=40$  is considered. External disturbance of  $-50$  kN is considered at the mid-span (at 7<sup>th</sup> node) of the beam in all cases while spinning at an angular velocity of  $100$  rad/sec. Displacement curves of the shaft both with and without rotation are shown in Fig.(9). It has been found that rotation effect increases the deformation of the shaft further. Observing the figures for different ply orientation shows that the effect of orientation angle is significant. Percentage difference of max displacement, Fig.(9(h)), is found to be substantial with hoop plies. Fig. (10) shows the variation of the displacement curve of shaft with and without Brazier effect. It is found that if we neglect the cross sectional deformation, it may lead to wrong estimation of displacement of the drive shaft. Brazier effect is found to be more prominent for  $[0^\circ]_{10}$  and goes on decreasing in importance as the ply-layup angle increases. Therefore, optimal design of the ply to resist Brazier effect will be to choose higher angle of ply.

Since the bending stiffness depends on the unknown,  $\rho$ , an iterative procedure is require to determine it. Fig.(4) show the no. of steps required for convergence of  $\rho$  for the different ply layups,  $[\pm\theta]_s$ . It has been found that it converges faster for larger  $\theta$ .

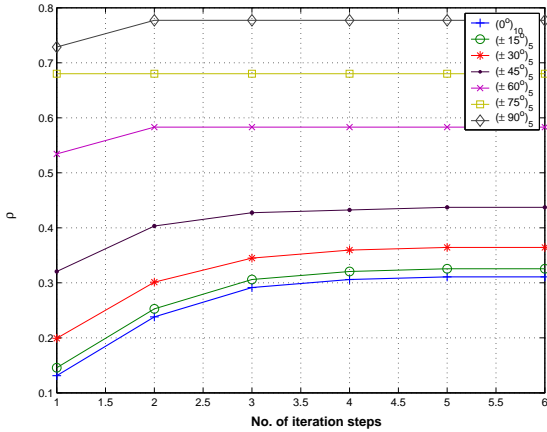


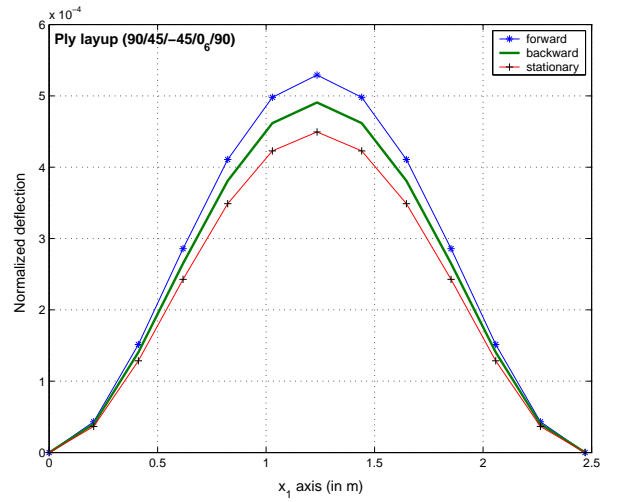
Fig 4. Convergence of nonlinear bending

### Natural frequencies and normal modes

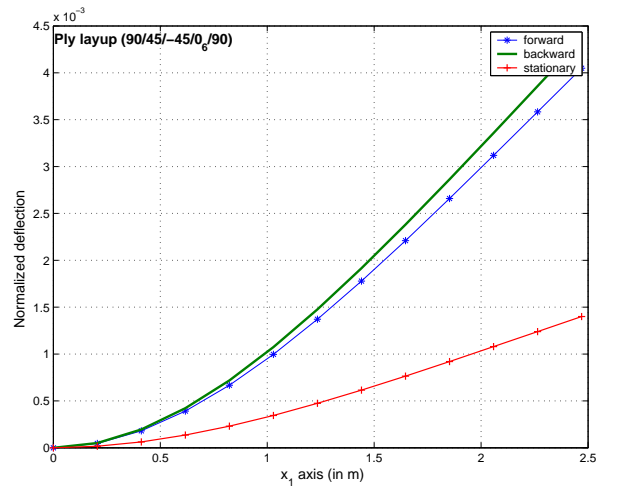
This section deals with the natural frequencies and mode shapes of the composite drive shafts as they are important structural dynamic characteristics and are required in the solution of resonant responses and for forced vibration analyses. Of particular interest here are practical situations pertaining to a spinning beam of finite length with clamped-clamped and clamped-free boundary conditions.

The free vibration response of stationary beams with general boundary conditions are well known, but for a spinning composite shafts have not been investigated by many researchers. Fig. (5) shows the results of numerical simulation for the mode shape of composite drive shafts spinning at  $60$  rad/sec, along with those of non-spinning shafts. It can be clearly observed that with rotation, deformation of the shaft increases further. As discuss in an earlier section, if a beam is put into a spinning motion, its natural frequencies split into two components: forward and backward precession. In case of cantilever (see Fig. (5)) it is observed that backward mode deflection exceeds those of the forward mode, and both precession mode shapes are far from that of the non-spinning shaft.

Graphite/Epoxy shaft of  $L=2.47$  m;  $R=63.45$  mm and  $t=1.321$  mm is considered for numerical simulation indicated in Fig.(5).



(a) clamped-clamped



(b) clamped-free

Fig 5. First Mode shape of forward and backward precession and of stationary composite drive shaft.

## Conclusion and Discussion

A beam model is presented in this work for a composite spinning shafts. Rotor blade analysis carried out previously by Hodges is extended here for the case of laminated composite shafts. Having validated with a few beam theories for shafts in the literature, the present continuum based shaft beam model can serve as a viable alternative for the vibration analysis of spinning laminated composite shafts. The governing equations obtained by this formulation are in a compact matrix form and are without any approximation in the geometry of the cross-section or the deformed beam reference line. The present finite element results match well with those in the literature. The critical speed of the composite laminated shaft is not always at the ply angle  $\theta = 0^\circ$ . It is dependent on the  $L/R$  ratio and the type of the boundary conditions. The composite shaft having a proper stacking sequence would have better dynamic performance than a conventional steel shaft. It has been found that rotation effect increases the deformation of the shaft further. Brazier effect which is believed to be important for high speed rotating shaft is found to be significant for the case when shaft is transmitting large uniform torque. It is found that there is not much cross-sectional deformation for the case of the first critical speed. Both forward and backward precession mode shapes is also capture for spinning drive shafts. It is also found that distinction between forward and backward precession becomes more obvious at higher modes and at larger spinning speeds. Another feature which is expected is that the more restrained a boundary condition represents, the closer are its forward and backward precession curves to that of the non spinning shaft.

## References

- 1 Bryan, G.H., "On the beats in the vibration of a revolving cylinder or bell," Proceedings of the Cambridge Philosophical Society, Vol. 7, 1890, pp. 101-111.
- 2 Dimentberg, F.M., "Flexural vibrations of rotating shafts," Butterworths, London, 1961.
- 3 Anderson, R.A., "Flexural vibration of uniform beams according to the Timoshenko theory," ASME Journal of Applied Mechanics Vol 20, 1953, pp. 504-510.
- 4 Trail-Nash, R.W. and Collar, A. R., "The effect of shear flexibility and rotatory inertia on the bending vibration of beam," Quarterly Journal of Mechanics and Applied Mathematics Vol. 6, 1953, pp. 186-222.
- 5 Huang, T.C., "Effect of rotatory inertia and of shear deformation on the frequency and normal mode equations of uniform beams with simple end conditions," ASME Journal of Applied Mechanics Vol. 28, 1961, pp. 579-584.
- 6 Bauer, H. F., "Vibration of rotating uniform beam," Journal of sound and vibration, Vol. 72, 1980, pp.177-189.
- 7 Greenberg, J. B. and Stavsky, Y., "Vibrations of laminated filament-wound cylindrical shells," AIAA Journal, Vol. 19, 1981, pp.1055-1062.
- 8 Rand, O. and Stavsky, Y., "Free vibration of spinning composite cylindrical shells," International Journal of Solids and Structures, Vol. 28, 1991, pp. 831-834.
- 9 Bert, C. W. and Kim, C. D., "Whirling of composite-material driveshafts including bending-twisting coupling and transverse shear deformation," Journal of Sound and Vibration, Vol. 117, 1995, pp.17-21.
- 10 Singh, S. P. and Gupta, K., "Composite shaft rotordynamic analysis using a layerwise theory," Journal of Sound and Vibration, Vol. 191(5) 1996, pp. 739-756.
- 11 Chen, L. W. and Peng, W. K., "The stability behavior of rotating composite shafts under axial compressive loads," Composite Structures, Vol. 41, 1998, pp.253-263.
- 12 Chang, M. Y., Chen, J. K. and Chang, C. Y., "A simple spinning laminated composite shaft model," International Journal of Solids and Structures, Vol. 41, 2004, pp.637-662.
- 13 Brazier, L. G., "On the flexure of and 'thin' cylindrical shells and other thin sections," Proc. Roy. Soc. London Ser. A, Vol. 116, 1927, pp. 104-114.
- 14 Harursampath, D. and Hodges D. H., "Asymptotic analysis of the non-linear behavior of long anisotropic tubes," International Journal of Non-Linear Mechanics, Vol. 34(6), November 1999, pp. 1003-1018.
- 15 Berdichevskii, V. L., "Variational-asymptotic method of constructing a theory of shells," PMM Vol. 43, No.4, 1979, pp. 664-687.
- 16 Kane, T. R. and Levinson, D. A., "Dynamics: Theory and Applications, Chapter 6," McGraw-Hill, Scarborough, C A., 1985.
- 17 Hodges, D. H., "A mixed variational formulation based on exact intrinsic equations for dynamics of moving beams," International Journal of Solids and Structures, Vol. 26(11), 1990, pp. 1253-1273.
- 18 Danielson, D. A. and Hodges, D. H., "A beam theory for large global rotation, moderate local rotation, and small strain.," Journal of Applied Mechanics, Vol. 55, 1988, pp. 179-184.
- 19 Hodges, D. H., Shang, X. and Cesnik, C. E. S., "Finite element solution of nonlinear intrinsic equations for curved composite beams," Journal of the American Helicopter Society Vol. 41(4), Oct. 1996, pp. 313 - 321.
- 20 Zinberg, H. and Symonds, M. F., "The Development of an Advanced Composite Tail Rotor Driveshaft," Presented at the 26th Annual Forum of the American helicopter Society, Washington, DC, June. 1970, pp 1-14.
- 21 Dos Reis, H. L. M., Goldman, R. B. and Verstrate, P. H., "Thin-walled laminated composite cylindrical tubes: Part III-Critical speed analysis," Journal of Composites Technology and Research. Vol. 9, pp. 22-36.

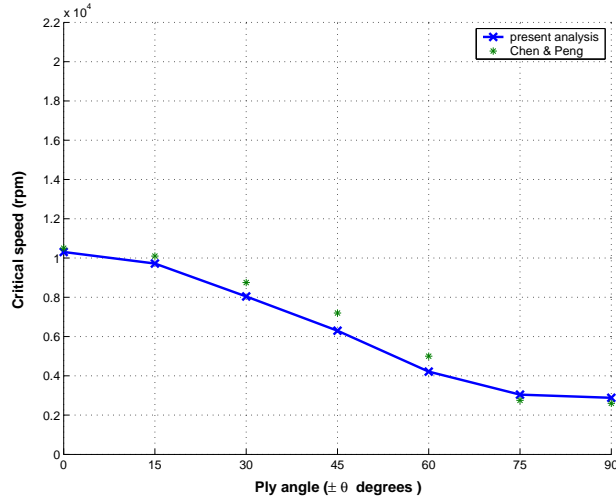


Fig 6. Critical speed vs. ply angle for L/R=40

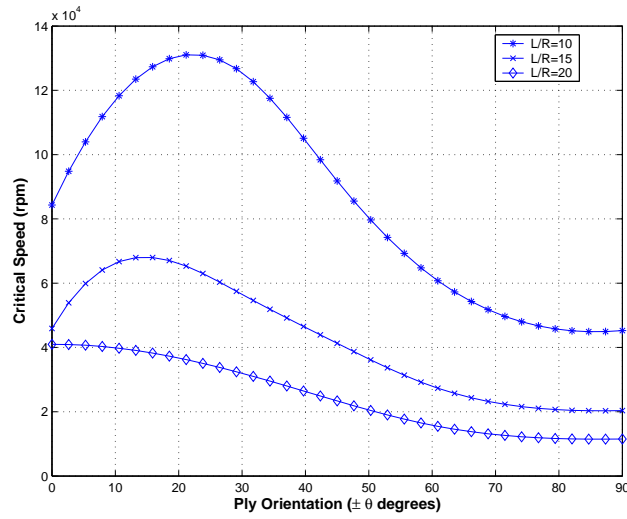
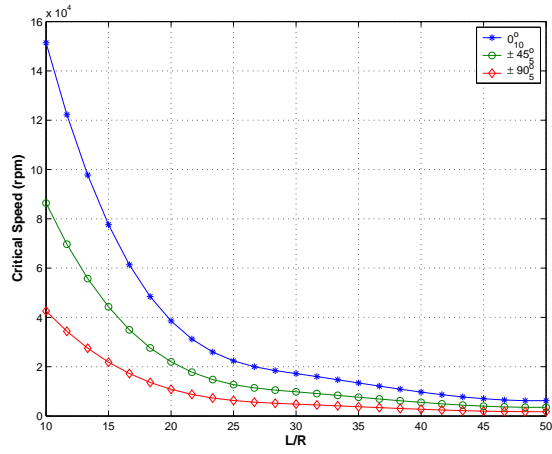


Fig 7. Critical speed vs. ply angle for various L/R ratios

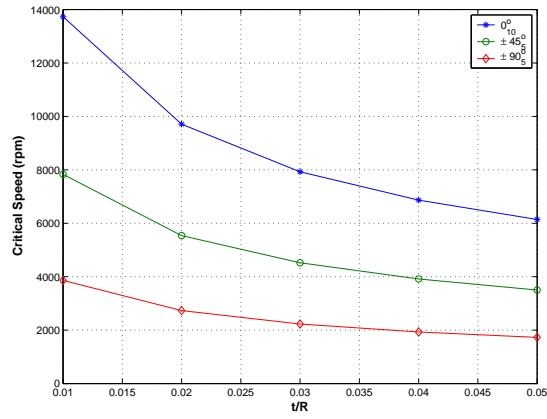
Investigator	Method of determination	Critical speed
Zinberg and Symmonds	Theoretical	5780
Bert	Bernoulli-Euler beam theory	5919
Bert and Kim	Bresse-Timoshenko beam theory	5714
Henrique dos Reis	FEM with beam element	4950
Present	MFEA with non-linear bending	5195

TABLE II

COMPARISON OF CRITICAL SPEED OF A COMPOSITE DRIVE SHAFT REPORTED BY DIFFERENT RESEARCHERS

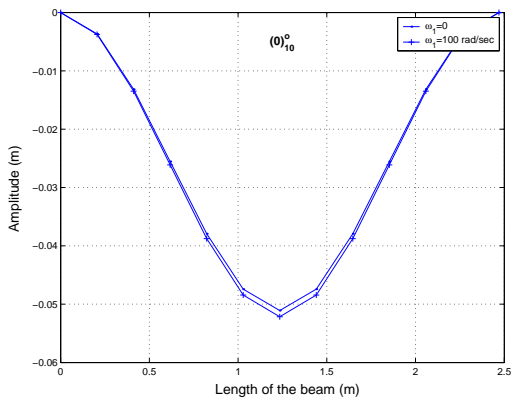


(a)

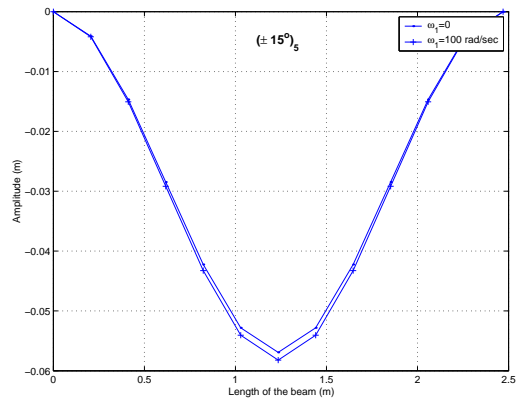


(b)

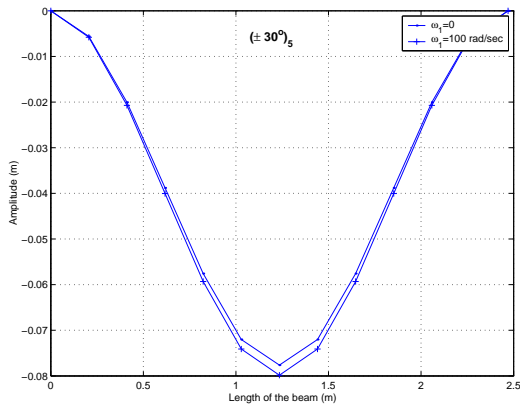
Fig 8. Critical speed vs. the (a) L/R ratio for different ply-layups and (b) t/R ratio for different ply layups



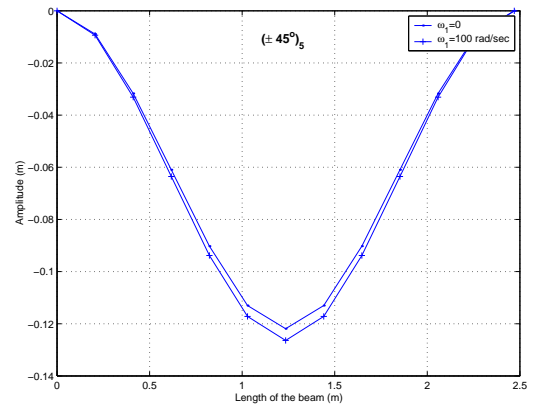
(a)



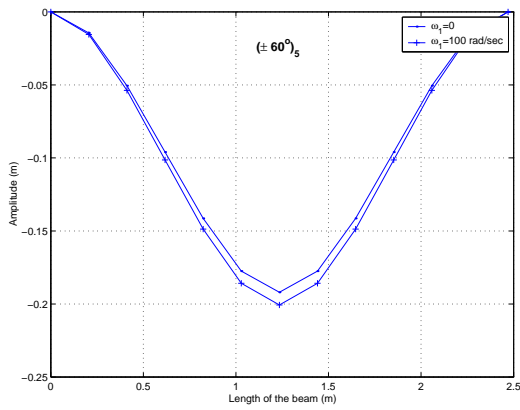
(b)



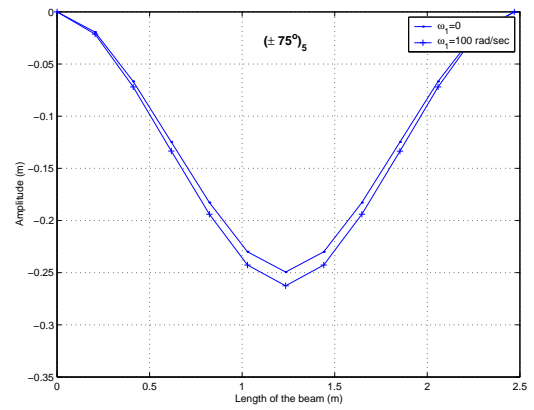
(c)



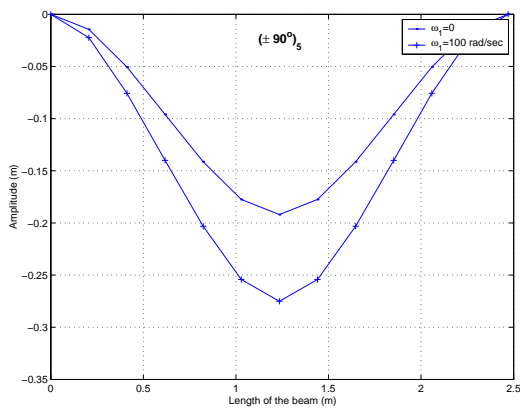
(d)



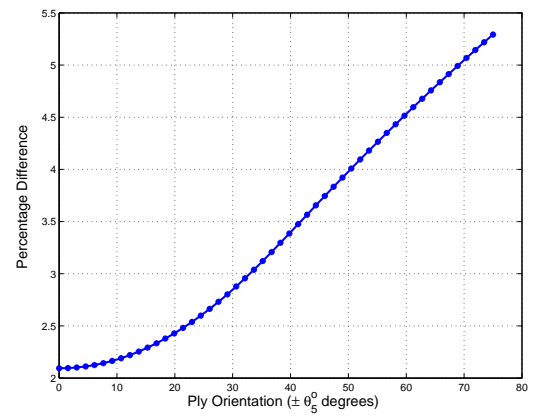
(e)



(f)



(g)



(h)

Fig 9. (a)-(g) Displacement curves of shafts with (-+-) and without (-) rotation and (h) maximum percentage difference ( in displacement with and without rotation) vs the ply orientation

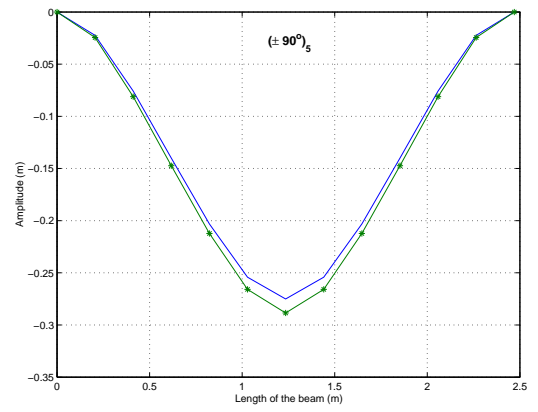
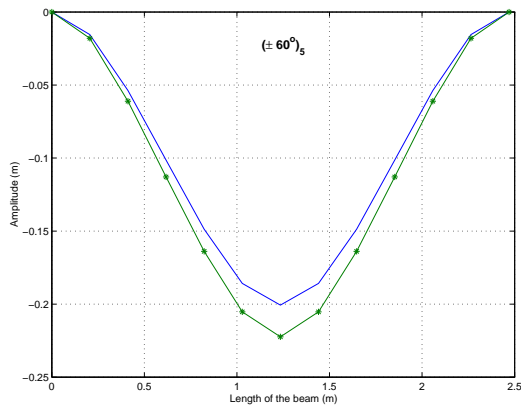
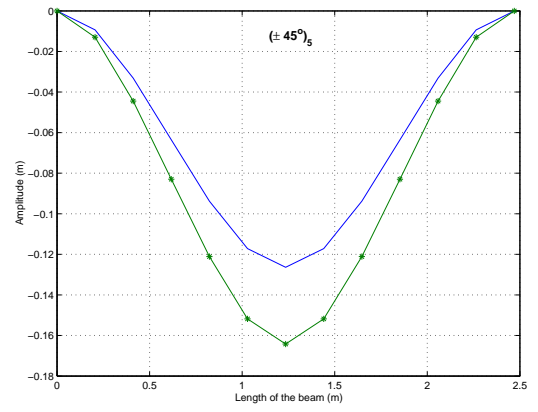
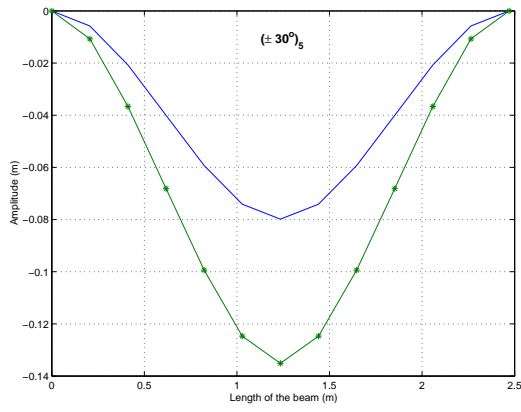
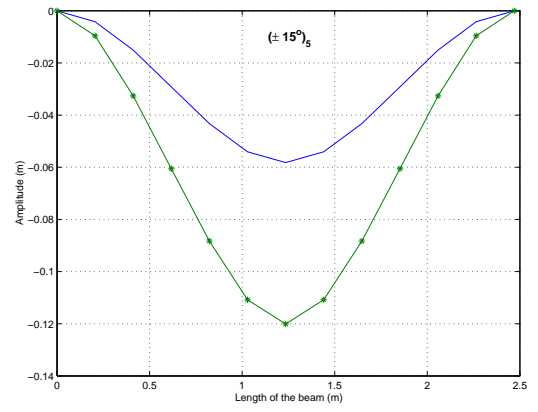
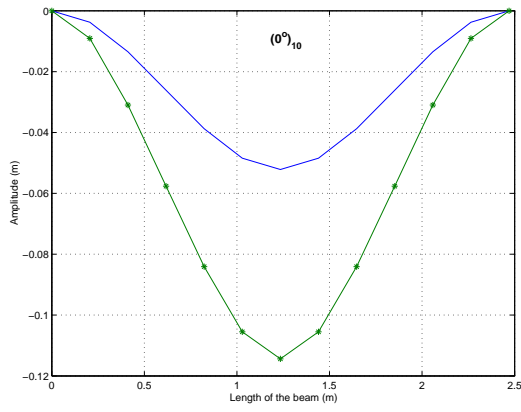


Fig 10. (a)-(f) Displacement curves for different ply orientations with (-\*-) and without (-) Brazier effect